Sensors and Actuators B 160 (2011) 1282–1287

Contents lists available at SciVerse ScienceDirect

Sensors and Actuators B: Chemical

journal homepage: www.elsevier.com/locate/snb

Enzyme mimic of heterobimetallic Cu(II) and Fe(III) tetrapyridylporphine modified nanoparticles

Mariana Hamer, Romina R. Carballo[1], Irene N. Rezzano*,[1]

Departamento de Química Analítica y Fisicoquímica, Facultad de Farmacia y Bioquímica, Universidad de Buenos Aires-CONICET, Junín 956, CP 1113 Buenos Aires, Argentina

ARTICLE INFO

Article history:
Received 10 May 2011
Received in revised form
20 September 2011
Accepted 21 September 2011
Available online 28 September 2011

Keywords:
Gold nanoparticles
Heterobimetallic porphyrin complexes
Enzyme mimics

ABSTRACT

The covalent binding of the porphyrin to immobilized gold nanoparticles resulted in a very useful and simple method to evaluate the absorption spectroscopy of a monolayer of porphyrins and the spectral changes produced by additional ligands.

The layer by layer deposition showed no distinguishable porphyrin-related absorption bands whereas the direct simultaneous binding of porphyrins (Cu(II) and Fe(III) tetrapyridylporphine) to immobilized gold nanoparticles showed a significantly higher absorption band at 412 nm corresponding to the Soret band of the porphyrin ring.

The ATR-FTIR spectra showed typical absorptions bands of porphyrin core at around 1000 cm^{-1} and 800 cm^{-1}, which were only observed in the Cu(II) complex of TPyP/AuNPs–APTES/SiO_2 suggesting that the CuTPyP molecule is tilted with respect to the substrate surface. The presence of FeTPyP produces changes in the geometry of the adsorbed CuTPyP porphyrins, indicating a flat accommodation of the porphyrinic rings in FeTPyP–CuTPyP composite that could be the reason of the differential tendency to include H_2O_2 as ligand. The difference UV–visible spectra of the bimetallic structures showed a very sensitive response to H_2O_2 concentration with a Kapp 3.75×10^3 M^{-1}(R: 0.9865; Std E: 2.6×10^{-2}) which was notoriously similar to K_m value for peroxidase enzyme (2.5×10^3 M^{-1}).

1. Introduction

The porphyrins and metalloporphyrins are important π-conjugated compounds with specific optical properties that can be easily modulated through the variation in molecular symmetry, metal coordination, dipole moment and extent of conjugation of the π-systems. For this reason, they have been widely used in the design of electrochemical and optical analytical devices with a number of applications [1–3].

Our research has been focused on biomimetic catalytic systems based on porphyrins where the combination of two different transition metal complexes resulted in more active catalysts than their mononuclear counterparts. A number of dinuclear complexes have been investigated to activate small molecules [4] but undoubtedly the synthetic Fe porphyrins as biomimetic analogs of the heme/Cu site of cytochrome *c* oxidase was the most intensively studied [5]. The synthetic dinuclear copper and iron systems have been decisive to the understanding of dioxygen binding and showed excellent results in catalysis attempting to design mimics of enzymes [6–8].

In previous reports, we studied the catalytic activity for molecular oxygen and hydrogen peroxide reduction of bimetallic porphyrin films as electrode modifiers [9–11]. A significantly high amperometric response to H_2O_2 was observed in certain bimetallic films of porphyrins, Fe(III) and Cu(II), confined to the electrode surface. This unique catalytic activity was not observed in monometallic species, and could be attributed to some synergic effect between the two metal complexes. The absorption spectroscopy was unable to corroborate this idea, since the porphyrinic B and Q bands were not affected by H_2O_2 concentration in the bimetallic system described.

Nanostructured metal films, excited by visible light, show localized surface plasmon oscillations resulting in the enhancement of local electromagnetic fields close to the metal surface [12–14]. This property, which is size and shape dependent, has been widely studied and exploited in numerous optical applications. In terms of the analytical point of view, the surface plasmon oscillations serve to monitor the interaction with surface-bound molecules [15]. In this line of research, it has been described that metalloporphyrin self-assembled films chemisorb on gold as tightly bound monolayers have properties consistent with a coplanar orientation of the macrocycle and can be optically monitored [16,17]. Additionally, porphyrin protected gold nanoparticles (AuNPs) with the aromatic macrocycle parallel to the AuNPs surface show drastic changes in

---

* Corresponding author.
E-mail address: irezzano@ffyb.uba.ar (I.N. Rezzano).

[1] CONICET permanent staff.

0925-4005/$ – see front matter © 2011 Elsevier B.V. All rights reserved.
doi:10.1016/j.snb.2011.09.063

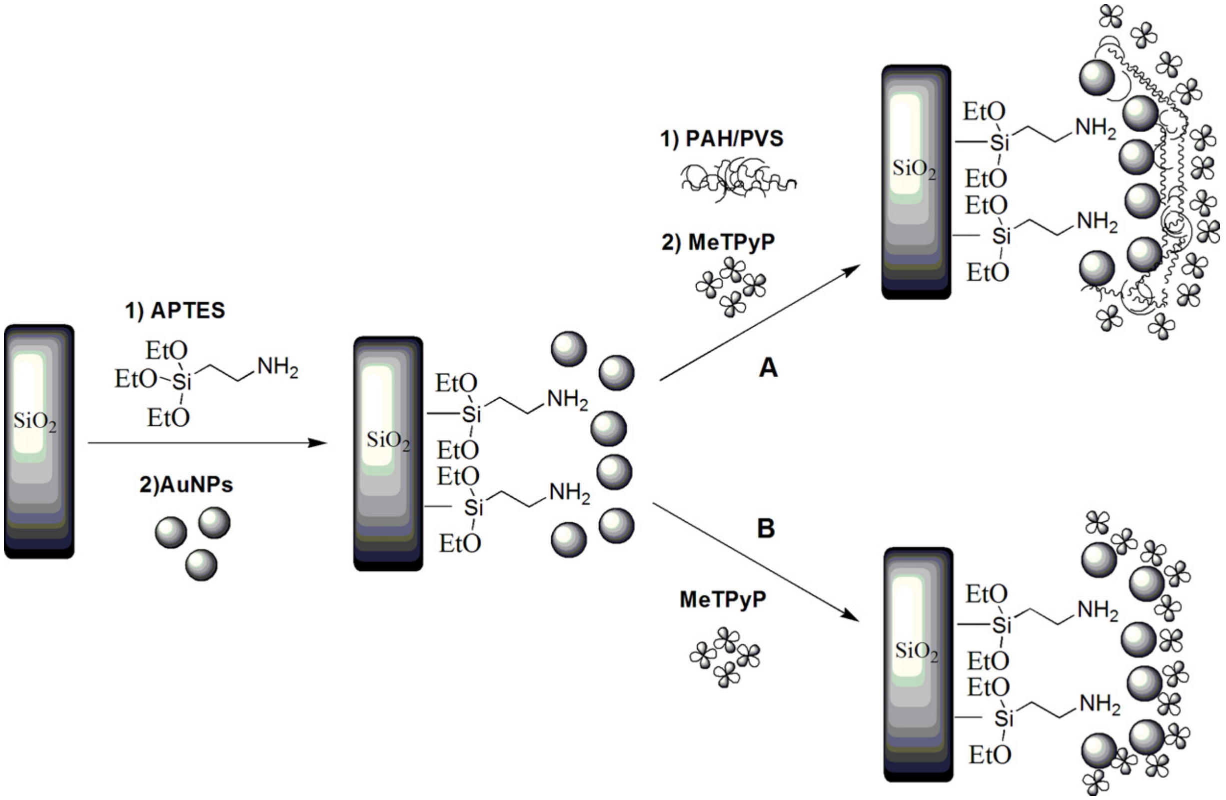

Scheme 1. Schematic representation of the assembly procedure onto SiO_2 surface: (a) APTES self assembled monolayer; (b) adsorption of gold nanoparticles (AuNPs); (c) FeTPyP and CuTPyP adsorption.

the absorbance spectra from modification of the electronic state of the porphyrin [18].

With these ideas in mind, we hypothesize that the high extinction coefficient of porphyrin (>200,000 $cm^{-1} M^{-1}$) must be reinforced by the increased coupling of the molecular π system in nanoparticles allowing us to evaluate the spectral changes produced by H_2O_2 inclusion on the bimetallic center.

Here, we report the synthesis and characterization by FTIR and SEM of immobilized gold nanoparticles modified with bimetallic films of porphyrins [Cu(II) and Fe(III) tetrapyridylporphine]. The metalloporphyrins were immobilized through layer-by-layer (LbL) deposition or by direct binding of the porphyrin ring to the nanoparticles by pyridine nitrogens [19].

We compare both systems by absorption spectroscopy as sensing material to follow the hydrogen peroxide reduction.

2. Material and methods

2.1. Reagents

Pre-cleaned glass slides (Iwaki Clinical Test Ware, Tokyo, Japan) used for UV–visible transmission measurements were cleaned with a “piranha solution” (H_2SO_4:H_2O_2 = 3:1), followed by flushing with plentiful water and purging with nitrogen gas.

Analytical grade gold (III) chloride trihydrate salt, poly(vinyl sulfonic acid) sodium salt, poly(allylamine hydrochloride) (Aldrich) and sodium citrate were used as supplied.

Fe(III) and Cu(II) complexes of 5,10,15,20-tetra(4-pyridyl)-21H,23H-porphine were prepared according to standard procedure [9,10]. 3-Amino propyl-triethoxy silane (APTES) was purchased from Fluka. All other reagents were obtained from Merck and used as received. Water was deionized and filtered using a Millipore water purification system (18 MΩ).

2.2. Apparatus

A HP8452 diode array spectrophotometer and a quartz crystal cell were used to obtain the UV spectra.

Particle size was verified by TEM. Gold nanoparticles in aqueous dispersion were imaged in a Phillips CM200 Transmission Electron Microscope after placing drops of dispersion onto gold grids, 400 mesh (SPI, PA, USA), and allowing the liquid to dry in air at room temperature (not shown). The scanning electron micrographs of the modified surfaces were obtained using a Zeiss DSM982 GEMINI SEM with Field Emission Gun (FEG), operated at 3 kV.

FTIR spectra were recorded with a Nicolet 6700 ThermoScientific, diamond crystal was used for ATR experiments. By subtracting the spectrum of the AuNPs–APTES–SiO_2 in the same conditions without porphyrins, the resulting spectrum was obtained. All spectra were baseline corrected.

2.3. Synthesis of gold nanoparticles

Gold nanoparticles were synthesized by a modification of the Turkevich method [20]. In brief, 4.5 mg of gold (III) chloride trihydrate ($HAuCl_4 \cdot 3H_2O$) was dissolved in 45 mL of MilliQ water, and 10 mL of this solution was brought to boil in a round-bottom flask under stirring. A 1.6 mL portion of a 1% sodium citrate solution was added to the solution using a stirrer. The solution turned red after 5 min, and the intensity of the color increased with time. Boiling was maintained for 20 min after which the heat was removed and stirring was continued for 15 min. Then, 8 mL of the nanoparticle suspension were centrifuged in 1.5 mL Eppendorf tubes at 7000 rpm (4.500 g) during 45 min to remove excess reducer; the supernatant was removed, and the remaining AuNPs were redispersed in 4 mL of MilliQ water.

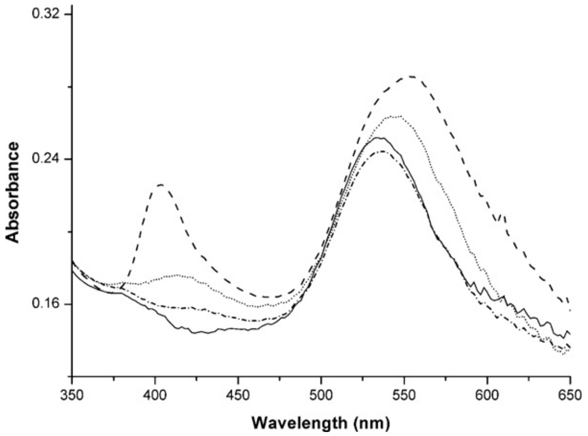

Fig. 1. Absorbance spectra of: AuNPs–APTES/SiO_2 (solid); PAH–PVS/AuNPs–APTES/SiO_2 (dash–dot); FeTPyP–CuTPyP/PAH–PVS/AuNPs–APTES/SiO_2 (dot); FeTPyP–CuTPyP/AuNPs–APTES/SiO_2 (dash).

2.4. Surface modification

Prior to use, SiO_2 plates were cleaned in "piranha" solution. The clean glasses were then immersed into a 10% (v/v) solution of APTES in ethanol for 6 h, rinsed extensively with ethanol, dried in N_2 stream and in a 60 °C oven for 6 h. Next, the silane functionalized surfaces were placed into the AuNPs suspension for 12 h to form a monolayer. After this time period, the substrates were removed from the NPs suspension and copiously rinsed with H_2O. Then they were immersed in MeTPyP solution at pH 2, for 12 h.

The LbL deposition was done by alternative immersion of the SiO_2 plates in poly(allylamine) (PAH) solution 1 mM and PVS 1 mM during 1 h each. Finally the modified substrates were immersed in MeTPyP for 12 h.

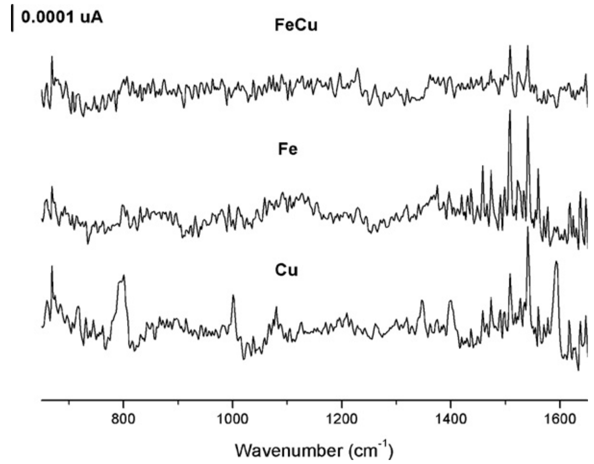

Fig. 3. ATR spectra of MeTPyP/AuNPs–APTES/SiO_2 (64 scans and 4 resolution).

The absorption spectra were obtained at pH 7. The modified glasses were immersed in MQ water (3 mL) and successive aliquots of 50 μL H_2O_2 (20 mM) or $NaNO_2$ (105 mM) were added.

3. Results and discussion

3.1. Synthesis and characterization of porphyrin nanoparticles composites

In order to find the best optical sensor architecture to evaluate ligand binding on immobilized metalloporphyrins, we prepared immobilized gold nanoparticles on a transparent substrate by attachment to APTES-coated glass (SiO_2) surface: AuNPs–APTES/SiO_2. This array was modified with metalloporphyrins (MeTPyP), Cu(II) and Fe(III) tetrapyridylporphine, by two different pathways: (a) through layer-by-layer (LbL) electrostatic deposition of the films poly(vinyl sulfonate) (PVS), poly(allylamine)

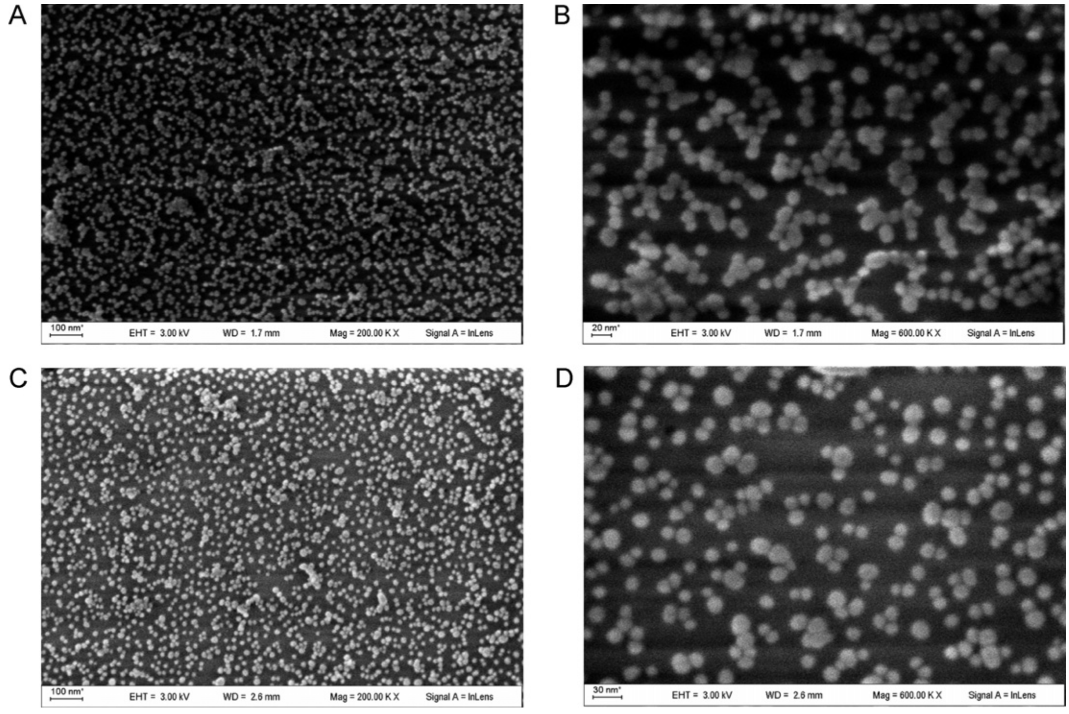

Fig. 2. SEM images (magnification 200k× – left – and 600k× – right –) of (A and B) AuNPs–APTES/SiO_2, mean size distribution 15 ± 5 nm and (C and D); MeTPyP/AuNPs–APTES/SiO_2, mean size distribution 17 ± 6 nm.

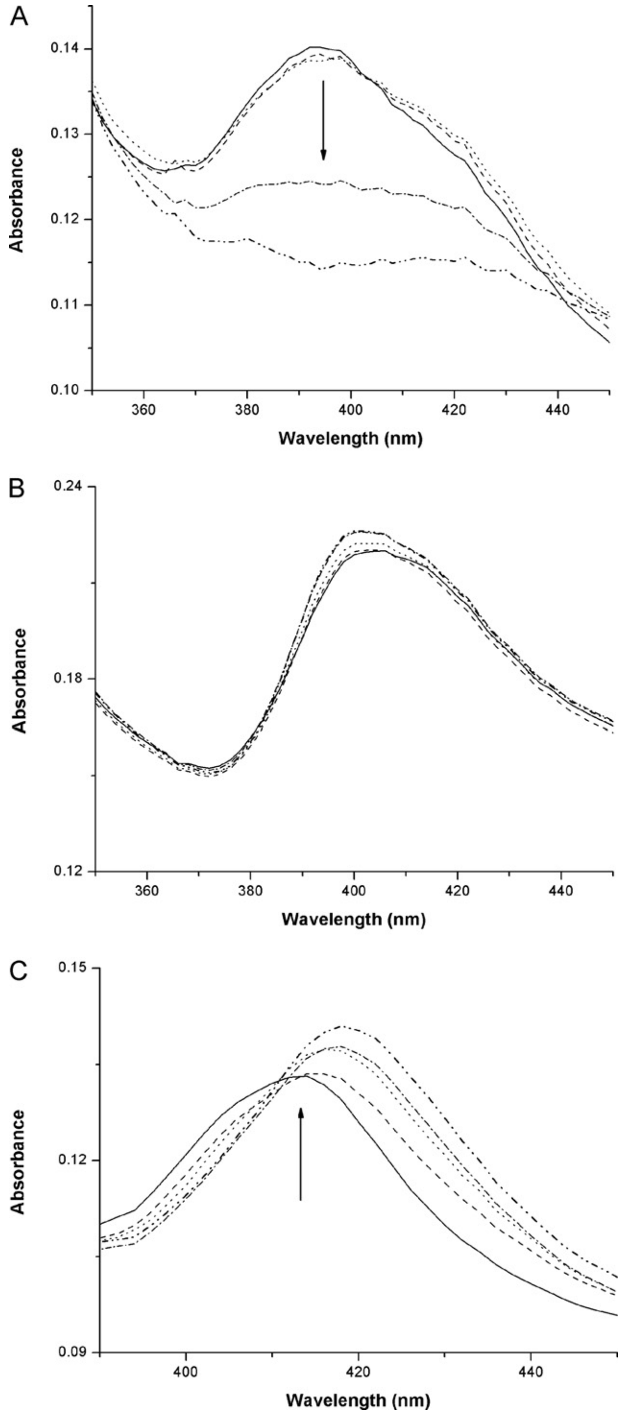

Fig. 4. Absorbance spectra of: FeTPyP/AuNPs–APTES/SiO_2 (A); CuTPyP/AuNPs–APTES/SiO_2 (B) and FeTPyP–CuTPyP/AuNPs–APTES/SiO_2 (C), after successive additions of 50 μL H_2O_2 (20 mM).

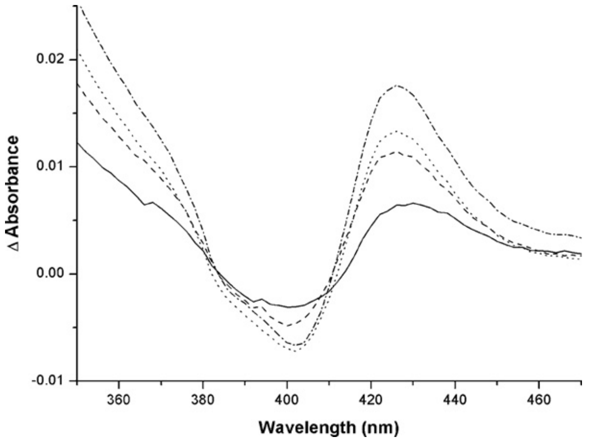

Fig. 5. Difference spectra between FeTPyP–CuTPyP/AuNPs–APTES/SiO_2 + H_2O_2 (successive additions of 50 μL H_2O_2 20 mM) and FeTPyP–CuTPyP/AuNPs–APTES/SiO_2.

hydrochloride (PAH) and metalloporphrins, and (b) by the direct binding of the porphyrin ring to the nanoparticles. Scheme 1 shows the sequence of immobilization.

In spite that the layer-by-layer growth method has been reported as a general route to compositionally modulated porphyrin films [21], the UV–visible spectra (Fig. 1, dot) does not show any clearly distinguishable porphyrin-related absorption bands, being completely dominated by the intense SP absorption of the gold nanocore. This result can be explained by the swelling effect of poly(allylamine) hydrochloride at pH 2 [22] or to a low amount of porphyrin labeling the outer polymer layer, however, the presence of porphyrin core became evident through the observation of its typical emission spectra (not shown). On the contrary, the covalent binding of the porphyrin to the gold surface [23] was very useful to evaluate the absorption spectroscopy since a significant higher band at 412 nm corresponding to the Soret band of the porphyrin ring was observed (Fig. 1, dash) and attributed to the increased coupling of the molecular π system ($\theta \sim 0$) of porphyrins in this arrangement [24].

The SEM images (Fig. 2) reveal the morphology and order degree of AuNPs–APTES/SiO_2 (Fig. 2A and B) and the composite films (Fig. 2C and D). A dense and uniform distribution of nanoparticles on the glass substrate can be observed. The composite MeTPyP/AuNPs–APTES/SiO_2 maintains a similar morphological distribution and shows a 2 nm larger mean diameter, consistent with a monolayer of porphyrins deposited on gold nanoparticle [25].

3.2. *ATR-FTIR*

The mid-frequency (650–2000 cm^{-1}) spectra of the immobilized nanoparticles are shown in Fig. 3. We focus on features key to the present studies: (a) the two absorptions bands that distinguish the porphyrin core at around 1000 cm^{-1}, in-plane pyrrole ring breathing mode, and at 800 cm^{-1}, which is due to an out-of-plane β-pyrrole-hydrogen deformation [25] and (b) the C=N axial deformation of pyridyl moiety in TPyP [26] band at 1590 cm^{-1} which is also evident in the spectra. The appearance of the above mentioned bands is only observed in the Cu(II) complex of TPyP/AuNPs–APTES/SiO_2 suggesting that the CuTPyP molecule is tilted with respect to the substrate surface. Additional pyridine ring stretching modes at 1510 and 1570 cm^{-1} are observed in the FeTPyP/AuNPs–APTES/SiO_2, which points to a perpendicular or at least tilted orientation of pyridyl moiety with respect to the gold surface in this film, with a flat or parallel orientation of the porphyrin core. Interestingly, the presence of FeTPyP produces changes in the geometry of the adsorbed CuTPyP porphyrins, since no porphyrin moiety bands are observed in the bimetallic structure. This last result indicates a flat accommodation of the porphyrinic rings in FeTPyP–CuTPyP composite that could be the reason of the differential tendency to include H_2O_2 as ligand.

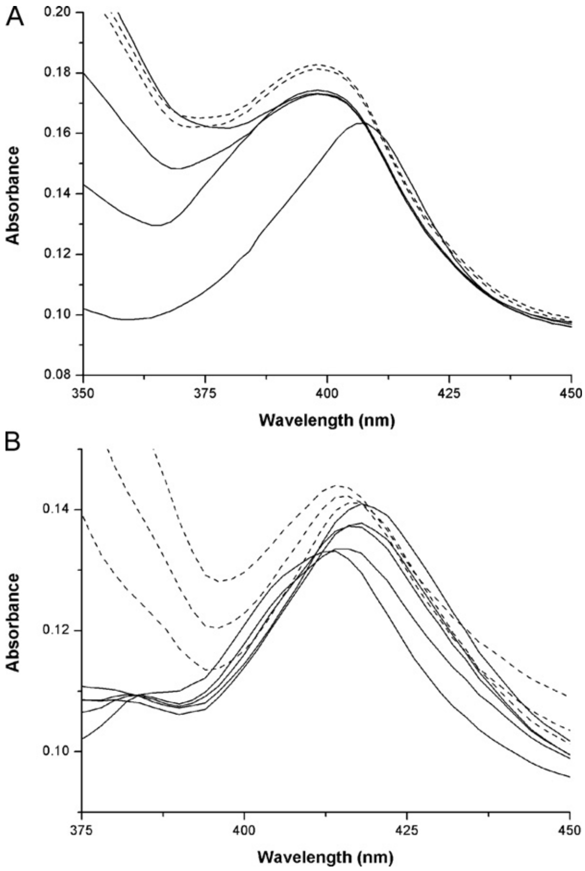

Fig. 6. Absorbance spectra of FeTPyP–CuTPyP/AuNPs–APTES/SiO_2: after successive additions of 50 μL $NaNO_2$ 105 mM (solid) and then additions of 50 μL H_2O_2 20 mM (dot) (A); and of 50 μL H_2O_2 20 mM (solid) and then additions of 50 μL $NaNO_2$ (dot) 105 mM (B).

3.3. Hydrogen peroxide effect on absorption spectroscopy

We performed the UV–visible spectra of the monometallic and bimetallic composites after successive additions of H_2O_2, in order to understand the interaction of hydrogen peroxide with the immobilized porphyrins. Fig. 4 shows these results: the Soret band of the FeTPyP deposited on gold nanoparticles showed a significant decrease upon addition of H_2O_2 (Fig. 4A) due to the deleterious effect of hydrogen peroxide on the aromatic ring whereas the CuTPyP absorption spectra did not change (Fig. 4B). Interestingly, the red shifted Soret band (around 412 nm) increased steadily with the addition of hydrogen peroxide (Fig. 4C) only in the bimetallic composites. These results are consistent with previous electrochemical experiments, confirming the synergic effect between the two metal complexes [9,10].

Considering that the Soret bands in the composite materials are very broad, because they are dominated by the low-spin heme center, we evaluate the difference spectra of the bimetallic structure which showed a linear response to H_2O_2 concentration (Fig. 5). Absorption spectral titration of heterobimetallic complex was performed by varying the final concentration of the H_2O_2 (0.5–2 mM). The experimental data adequately fits to the following equation (R: 0.9865; Std E: 2.6×10^{-2}) [27,28], which was used to calculate the intrinsic binding constant, Kapp,

$$\frac{1}{A_{\text{obs}} - A_0} = \frac{1}{A_c - A_0} + \frac{1}{K_{\text{app}}(A_c - A_0)[H_2O_2]} \quad (1)$$

where $[H_2O_2]$ is the final concentration of hydrogen peroxide, A_c is the absorbance of the complex (maxima absorbance at 428 nm) and A_0 is the initial absorbance (without addition of H_2O_2).

A Kapp 3.75×10^3 M^{-1} was obtained by this experimental system, which is very close to the value reported for the peroxidase enzyme (2.5×10^3 M^{-1}) [29]. This result strongly suggests that the bimetallic composite accommodates in a favorable geometry to include hydrogen peroxide as ligand.

The Soret band shifted hypsochromically by 10 nm (Fig. 6A) upon the addition of sodium nitrite to the immobilized metalloporphyrins composite, indicating that the bimetallic complex coordinates nitrogen monoxide through the nitrogen atom to form nitrosyl derivative. This complex is very stable and cannot be displaced for increasing concentration of H_2O_2 (Fig. 6A). Conversely, and indicating a lower affinity, the H_2O_2 adduct can be displaced by addition of sodium nitrite (Fig. 6B).

Absorbance at Söret band (412 nm) showed a linear range response with increasing hydrogen peroxide concentration up to 1.5 mM. The linear regression equation for Fe(III)TPyP–Cu(II)TPyP/AuNPs–APTES/SiO_2 is expressed as $A = 1 \times 10^{-5}$ M^{-1} $X + 0.1393$, $R2 = 0.9942$. The sensitivity for H_2O_2 detection is 1×10^{-5} M^{-1} (10 μM^{-1}) and the detection limit calculated is 0.15 mM. These values are very similar to those reported in literature for LSPR-based optical sensor [30–32].

4. Conclusions

The covalent linkage of the porphyrin to the gold surface was very useful to evaluate the absorption spectroscopy of the immobilized system. A significant higher peak at 412 nm was observed, which could be attributed to the coupling of the molecular π system ($\theta \sim 0$) to the gold substrate. SEM images showed a dense and uniform distribution of nanoparticles on the gold substrate, the composite MeTPyP/AuNPs–APTES/SiO_2 maintained a similar morphological distribution with a larger mean diameter (2 nm), probably due to the porphyrin deposition.

The presence of FeTPyP produced changes in the geometry of the adsorbed CuTPyP porphyrins resulting in the special accommodation of the porphyrinic rings in FeTPyP–CuTPyP composite that could be the reason of the differential tendency to include H_2O_2 from the observed in solution.

This method allowed us to observe the effect of a strong ligand, such as nitrite anion, which irreversibly affects the bimetallic complex.

Acknowledgements

Financial support from University of Buenos Aires (UBACyT), ANPCyT and CONICET are gratefully thanked. Mariana Hamer also thanks CONICET for a doctoral fellowship. The authors gratefully thank to Ulises Casado from INTEMA-CONICET.

References

[1] D. Wöhrle, G. Schnurpfeil, Porphyrins and phthalocyanines in macromolecules, in: K.M. Kadish, K.M. Smith, R. Guilard (Eds.), The Porphyrin Handbook, vol. 17, Academic Press, San Diego, 2000, p. 110.
[2] J.F. van Staden, R.I. Stefan-van Staden, Application of porphyrins in flow-injection analysis: a review, Talanta 80 (2010) 1598–1605.
[3] M. Biesaga, K. Pyrzyńska, M. Trojanowicz, Porphyrins in analytical chemistry. A review, Talanta 51 (2000) 209–224.
[4] E.K. van den Beuken, B.L. Feringa, Bimetallic catalysis by late transition metal complexes, Tetrahedron 54 (1998) 12985–13011.
[5] V.J. Selverstone, Dioxygen reactions, in: I. Bertini, H.B. Gray, E.I. Stiefel, V.J. Selverstone (Eds.), Biological Inorganic Chemistry, University Science Books, New York, 2007 (Chapter 5).
[6] J.P. Collman, R.A. Decreau, C. Zhang, Synthesis of cytochrome *c* oxidase models bearing a Tyr^{244} mimic, J. Org. Chem. 69 (2004) 3546–3549.

[7] J.P. Collman, S. Ghosh, Recent applications of a synthetic model of cytochrome *c* oxidase: beyond functional modeling, Inorg. Chem. 49 (2010) 5798–5810.

[8] J.P. Collman, R. Boulatov, C.J. Sunderland, V. Fu, Functional analogues of cytochrome *c* oxidase, myoglobin, and hemoglobin, Chem. Rev. 104 (2004) 561–588.

[9] J.M. Vago, V. CampodalÍ Orto, E. Forzani, J. Hurst, I.N. Rezzano, New bimetallic porphyrin film: an electrocatalytic transducer for hydrogen peroxide reduction applicable to first-generation oxidase-based biosensors, Sens. Actuators B 96 (2003) 407–412.

[10] M. Vago, V. Campodall'Orto, I. Rezzano, E. Forzani, E.J. Calvo, Metalloporphyrin electropolymerization: electrochemical quartz crystal microgravimetric studies, J. Electroanal. Chem. 566 (2004) 177–185.

[11] M. Hamer, R.R. Carballo, I.N. Rezzano, Electrocatalytic reduction of hydrogen peroxide by nanostructured bimetallic films of metalloporphyrins, Electroanalysis 21 (2009) 2133–2138.

[12] F. Scandola, C. Chiorboli, A. Prodi, E. Lengo, E. Alessio, Photophysical properties of metal-mediated assemblies of porphyrins, Coord. Chem. Rev. 250 (2006) 1471–1496.

[13] C. Burda, X. Chen, R. Narayanan, M.A. El-Sayed, Chemistry and properties of nanocrystals of different shapes, Chem. Rev. 105 (2005) 1025.

[14] N.P. Prasad, Nanophotonics, John Wiley & Sons, New York, 2004, p. 129.

[15] K.G. Thomas, P.V. Kamat, Chromophore-functionalized gold nanoparticles, Acc. Chem. Res. 36 (2003) 888–898.

[16] R. Gordon, D. Sinton, K.L. Kavanagh, A.C. Brolo, A new generation of sensors based on extraordinary optical transmission, Acc. Chem. Res. 41 (2008) 10494–11057.

[17] A. Yu, Z. Liang, J. Cho, F. Caruso, Nanostructured electrochemical sensor based on dense gold nanoparticle films, Nano Lett. 3 (2003) 1203–1207.

[18] M. Kanehara, H. Takahashi, T. Teranishi, Gold(0) porphyrins on gold nanoparticles, Angew. Chem. Int. Ed. 47 (2008) 307–310.

[19] C.M. Aikens, G.C. Schatz, TDDFT studies of absorption and SERS spectra of pyridine interacting with Au_{20}, J. Phys. Chem. A 110 (2006) 13317–13324.

[20] J. Kimling, M. Maier, B. Okenve, V. Kotaidis, H. Ballot, A. Plech, Turkevich method for gold nanoparticle synthesis revisited, J. Phys. Chem. B 110 (2006) 15700–15707.

[21] K. Araki, M.J. Wagner, M.S. Wrighton, Layer-by-layer growth of electrostatically assembled multilayer porphyrin films, Langmuir 12 (1996) 5393–5398.

[22] G. Jiang, A. Baba, H. Ikarashi, R. Xu, J. Locklin, K.R. Kashif, K. Shinbo, K. Kato, F. Kaneko, R. Advincula, Signal enhancement and tuning of surface plasmon resonance in Au nanoparticle/polyelectrolyte ultrathin films, J. Phys. Chem. C 111 (2007) 18687–18694.

[23] D.F. Yang, D. Bizzotto, J. Lipkowski, B. Pettinger, S. Mirwald, Electrochemical and second harmonic generation studies of 2,2′-bipyridine adsorption at the Au(1 1 1) electrode surface, J. Phys. Chem. 98 (1994) 7083–7089.

[24] H. Imahori, T. Umeyama, Technonlogies for nano-optical devices and systems, in: M. Ohtsu (Ed.), Series: Springer Series in Optical Sciences, Volume package: Progress in Nano-Electro Optics, Springer, London, 2010.

[25] L. Wei, H. Tiznado, G. Liu, K. Padmaja, J.S. Lindsey, F. Zaera, D.F. Bocian, Adsorption characteristics of tripodal thiol-functionalized porphyrins on gold, J. Phys. Chem. B 109 (2005) 23963–23971.

[26] L. Wang, Y. Fu, Z. Wang, Y. Fan, X. Zhang, Investigation into an alternating multilayer film of poly(4-vinylpyridine) and poly(acrylic acid) based on hydrogen bonding, Langmuir 15 (1999) 1360–1363.

[27] A. Kathiravan, R. Renganathan, Effect of anchoring group on the photosensitization of colloidal TiO_2 nanoparticles with porphyrins, J. Coll. Int. Sci. 331 (2009) 401–407.

[28] H.A. Benesi, J.H. Hildebrand, A spectrophotometric investigation of the interaction of iodine with aromatic hydrocarbons, J. Am. Chem. Soc. 71 (1949) 2703–2707.

[29] H. Penha Freire Maciel, C.M. Cação Paiva Gouvêa, M. Toyama, M. Smolka, S. Marangoni, G.M. Pastore, Extraction, purification and biochemical characterization of a peroxidase from *Copaifera langsdorffii* leaves, Quim. Nova 30 (2007) 1067–1071.

[30] P. Vasileva, B. Donkova, I. Karadjov, C. Dushkin, Synthesis of starch-stabilized silver nanoparticles and their application as a surface plasmon resonance-based sensor of hydrogen peroxide, Colloids Surf. A: Physicochem. Eng. Aspects 382 (2011) 203–210.

[31] X. Hu, S. Tao, An optical fiber H_2O_2-sensing probe using a titanium(IV) oxyacetylacetonate immobilized nafion coating on an bent optical fiber probe, IEEE Sens. J. 9 (2011) 2032–2036.

[32] J. Tashkhourian, M.R. Hormozi-Nezhad, J. Khodaveisi, R. Dashti, A novel photometric glucose biosensor based on decolorizing of silver nanoparticles, Sens. Actuators B 158 (2011) 185–189.

Biographies

M. Hamer obtained her B.Sc. in Pharmacy from the University of Buenos Aires in 2007. She is currently a graduate student at the Department of Analytical Chemistry and Physicochemical in the School of Pharmacy at the University of Buenos Aires, with Prof. Irene Rezzano as supervisor. Her research area is the design of phases with molecular recognition ability.

R.R. Carballo is a CONICET assistant researcher at the Department of Analytical Chemistry and Physicochemical in the School of Pharmacy at the University of Buenos Aires. She obtained her Ph.D. in Analytical Chemistry in 2007. Her research area is the development of electrochemical and optical sensors and biosensors.

I.N. Rezzano received her B.Sc. from University of Buenos Aires in 1977 and her Ph.D. in Chemistry in 1984. From 1985 to 1988 she was a Postdoctoral Fellow in Chemistry Department at the University of California, Davis. She is currently a full professor and research leader at the Department of Analytical Chemistry and Physicochemical in the School of Pharmacy at the University of Buenos Aires. Her research interest is the design of supramolecular structures with molecular recognition ability, containing metalloporphyrins as electrochemical/optical reactive group, for sensors and biosensors applications.